*American Mineralogist, Volume 82, pages 1063–1072, 1997*

# Viscoelastic relaxation measurements in the system $SiO_2$-$NaAlSiO_4$ by photon correlation spectroscopy

**RALF SIEWERT* AND MATTHIAS ROSENHAUER†**

Mineralogisch-Petrologisches Institut der Universität Göttingen, Goldschmidtstrasse 1, D-37077 Göttingen, Germany

## ABSTRACT

Relaxation times of longitudinal strain for five supercooled liquids along the join $SiO_2$ (qz)-$NaAlSiO_4$ (ne) including the compositions of albite (ab), $ab_{50}jd_{50}$, jadeite (jd), $jd_{66}ne_{33}$, and $jd_{33}ne_{66}$ were measured by photon correlation spectroscopy within the temperature and relaxation time ranges 711–1116 °C and 35–$2 \times 10^{-4}$ s, respectively. The measured time correlation functions are fitted to the Kohlrausch-Williams-Watts equation, $\Phi^l(t) = \exp(-t/\tau^l_{P,T})^\beta$, yielding isothermal relaxation functions for longitudinal strain at constant stress. The temperature dependence of the longitudinal strain relaxation times obeys an Arrhenian type equation. The relaxation of the longitudinal strain cannot be described by a single relaxation time but by a relaxation time distribution. The width of the relaxation time distribution, which is represented by the parameter β, is independent over a large temperature range, indicating thermorheological simplicity. The decrease of the parameter β corresponds to an increase of the excess (configurational) heat capacity with increasing (Na+Al) content, together indicating an increasing fragility of the supercooled liquids toward the composition of $NaAlSiO_4$. Increasing fragility is also shown from the activation energy obtained from longitudinal strain relaxation and shear viscosity measurements, which passes a minimum near 40 mol% $NaAlSiO_4$ at low temperatures but decreases toward $NaAlSiO_4$ composition at higher temperatures. A comparison between strain, stress, and enthalpy relaxation times shows clearly that the relaxation process resulting from a thermal pertubation is slower than from a mechanical perturbation.

## INTRODUCTION

Understanding the physicochemical properties of silicate liquids is important for improving numerical models of geodynamic processes, which require new or refined values for transport parameters such as diffusivity or viscosity. These transport parameters are essentially determined by the structure of a liquid and its dynamics. Moreover, the key to understanding the dynamic behavior of liquids lies in the determination of relaxation times of microscopic or macroscopic melt properties as a function of temperature and pressure (Dingwell and Webb 1990). In general, relaxation is a process of reorganization of the melt structure to reach thermodynamic equilibrium after a perturbation. It involves changes of the average molecular configuration, and the required time for this process is called the relaxation time, τ. Viscoelastic or mechanical relaxation is the response to a mechanical pertubation whereas structural relaxation is the response to a thermal pertubation (e.g., Scherer 1986; Mazurin 1986). In the former case the measurements are isothermal, whereas for the latter the response to a (continous) change in temperature is observed.

The isothermal viscoelastic relaxation can be measured with different techniques depending on the time scale of the relaxation process: For example, torsion measurements (longitudinal and shear stress relaxation times at constant strain) or pressure jump measurements (volume strain relaxation times at constant stress) are suitable for relaxation times above 10 s, whereas ultrasonic measurements (longitudinal and shear stress relaxation times at constant strain) are appropriate for the relaxation time range $10^{-6}$–$10^{-9}$ s. Photon correlation spectroscopy (PCS) closes the time gap between 10–$10^{-6}$ s left open by the previously mentioned methods. Here, the time dependence of the intensity of scattered light resulting from thermally driven density (strain) fluctuations contains information on the kinetics of longitudinal strain relaxation at constant stress.

To get a better understanding of the relationship between the structure of a melt and its dynamics, we made measurements of longitudinal strain relaxation on supercooled liquids in the system $SiO_2$ (quartz, qz)-$NaAlSiO_4$ (nepheline, ne) including compositions of vitreous albite (ab), $ab_{50}jd_{50}$, jadeite (jd), $jd_{66}ne_{33}$, and $jd_{33}ne_{66}$ using photon correlation spectroscopy. For many of these compositions, no data previously existed. We have chosen this

* Present address: Laboratoire de Physique et Mécanique des Géomatériaux, Université de Marne-la-vallée, 93166 Noisy le Grand cedex, France.

† Deceased February 10, 1996.

0003–004X/97/1112–1063$05.00

**TABLE 1.** Chemical composition (in wt%) of the glass samples

| | Batch no. | $SiO_2$ | $Al_2O_3$ | $Na_2O$ | CaO | MgO | $Fe_2O_3$ | FeO | $K_2O$ | MnO | $H_2O$ |
|---|---|---|---|---|---|---|---|---|---|---|---|
| ab* | B-6419 | 68.46(68.74) | 18.78(19.44) | 12.22(11.82) | 0.02 | <0.01 | n.d. | 0.043 | 0.016 | 0.029 | n.d. |
| $ab_{50}jd_{50}$† | bn-8833 | 65.1 (64.69) | 22.0 (21.96) | 13.45(13.35) | 0.007 | 0.01 | 0.006 | n.d. | 0.005 | n.d. | <0.001 |
| jd* | B-5560 | 59.86(59.45) | 25.52(25.22) | 14.58(15.33) | 0.018 | 0.004 | n.d. | 0.023 | 0.022 | 0.021 | n.d. |
| $jd_{66}ne_{33}$† | B-8959 | 55.2 (54.96) | 27.4 (28.01) | 17.08(17.03) | 0.059 | 0.011 | 0.013 | n.d. | 0.008 | n.d. | <0.001 |
| $jd_{33}ne_{66}$† | B-8960 | 50.2 (49.36) | 30.9 (31.49) | 19.25(19.14) | 0.013 | 0.031 | 0.013 | n.d. | 0.002 | n.d. | <0.001 |

*Note:* Theoretical stoichiometric composition indicated by values in parentheses. n.d. = not determined.
* Analysis by electron microprobe (Badia 1988, personal communication).
† Analytical methods: Spectral photometry for $SiO_2$, $Al_2O_3$, $Fe_2O_3$, and MnO; atomic absorption spectrometry for $Na_2O$, $K_2O$, CaO, and MgO, gravimetry for $H_2O$ and titration for FeO; total iron as $Fe_2O_3$ (analyst P. Mielke).

join, because the anionic melt structure resembles the tridymite-like structure of $SiO_2$ glass and is independent of composition (Taylor and Brown 1979). Furthermore, several studies in this system are available yielding shear viscosity data (see Mysen 1988; Stein and Spera 1993 for data compilation), from which shear stress relaxation times can be calculated. Enthalpy relaxation parameters are also present for supercooled $SiO_2$ liquid (Richet and Bottinga 1984) and supercooled albite liquid (Richet and Bottinga 1984; Martens et al. 1987). Parameters for strain and stress relaxation exist for $SiO_2$-glass and supercooled liquid (Mills 1974; Bucaro and Dardy 1977; Höfler and Seifert 1984) and supercooled jadeite liquid (Siewert and Rosenhauer 1994). We repeated the measurements on jadeite composition, because the experimental setup was improved yielding more precise data and a broader temperature range than our previous measurements (Siewert and Rosenhauer 1994). Furthermore, we compare our calculated activation energies with those obtained from shear viscosity measurements from Riebling (1966), Taylor and Rindone (1970), Cranmer and Uhlmann (1981), Urbain et al. (1982), N'Dala et al. (1984), Hummel and Arndt (1985), Knoche (1993), and Stein and Spera (1993) to explore the compositional dependence of the fragility of the liquids. Fragility is also discussed by comparing the excess heat capacity data of Richet and Bottinga (1984) and Martens et al. (1987) with our values of the relaxation parameter, $\beta$. Furthermore we compare the relaxation parameters of longitudinal strain, shear stress, and enthalpy relaxation and discuss the different behavior of liquids after a mechanical and a thermal perturbation.

## EXPERIMENTAL METHODS

### Starting materials

The experiments were performed on supercooled liquids with compositions of vitreous ab, $ab_{50}jd_{50}$, jd, $jd_{66}ne_{33}$, and $jd_{33}ne_{66}$. The glasses were prepared from high purity grade oxides by Schott Glaswerke, Mainz. The chemical analysis of the glasses are given in Table 1. With exception of composition $jd_{33}ne_{66}$ all samples contain a small amount of bubbles, which are less than 0.5 mm in diameter. Slabs of $5 \times 5 \times 12$ mm were cut from the glass and all faces were polished to highest optical quality to minimize parasitic scattered light.

### Photon correlation spectroscopy

The theory of PCS is described in detail elsewhere (e.g., Lai et al. 1975; Berne and Pecora 1976; Siewert and Rosenhauer 1994). Briefly, the time dependence of thermally driven density (strain) fluctuations is measured by recording the time correlation function of the fluctuations in the intensity of the scattered light with a digital autocorrelator when a laser beam propagates through a liquid. These density fluctuations grow and decay by the same mechanism that gives rise to the viscoelastic relaxation. They arise from isobaric fluctuations in the local entropy and from adiabatic fluctuations in the local pressure. Moreover, the density fluctuations are isothermal because they are much slower than the thermal diffusion time constant. The PCS measurements yield the isothermal relaxation function for longitudinal strain in response to changes in longitudinal stress $\Phi^l(t)$, which is related to the recorded time correlation function $G(t)$ by

$$G(t) = a(1 + b|\Phi^l(t)|^2) \tag{1}$$

with $a$ the measured baseline of the time correlation function and $b$ an adjustable parameter, depending on experimental conditions. The square of the relaxation function for longitudinal strain $|\phi^l(t)|^2$ is fitted to the Kohlrausch-Williams-Watts equation (Williams and Watts 1970)

$$|\Phi^l(t)|^2 = \exp\left(-\frac{2t}{\tau^l_{P,T}}\right)^\beta \tag{2}$$

where the relaxation time $\tau^l_{P,T}$ and the exponent $\beta$ are the fit parameter. The relaxation time superscript $l$ indicates longitudinal, while the subscripts $P$ and $T$ indicate constant stress and temperature, respectively. The parameter $\beta$ ranges from zero to one and controls the width of the relaxation time distribution. In case of $\beta = 1$, it exists only a single relaxation process with the relaxation time $\tau^l_{P,T}$. Because the relaxational behavior of most melt systems is dominated by more than a single relaxation process leading to a distribution of relaxation times ($\beta < 1$), the average relaxation time $\langle\tau^l_{P,T}\rangle$ of the different relaxation processes must be calculated by

$$\langle\tau^l_{P,T}\rangle \equiv \int_0^\infty |\Phi^l(t)|\,dt = (\tau^l_{P,T}/\beta)\Gamma(1/\beta) \tag{3}$$

with $\Gamma(1/\beta)$ the gamma function at $1/\beta$.

**TABLE 2.** Relaxation parameters $\tau'_{P,T}$, β, and $\langle\tau'_{P,T}\rangle$, resulting from Equations 2 and 3

| $T$, °C | $\tau'_{P,T}$, s | β | $\langle\tau'_{P,T}\rangle$, s | $T$, °C | $\tau'_{P,T}$, s | β | $\langle\tau'_{P,T}\rangle$, s |
|---|---|---|---|---|---|---|---|
| | **Albite** | | | | **$ab_{50}jd_{50}$** | | |
| 711 | 2.07E+01 | 0.55 | 3.47E+01 | 799 | 1.01E+01 | 0.56 | 1.67E+01 |
| 718 | 9.26E+00 | 0.61 | 1.34E+01 | 799 | 7.72E+00 | 0.57 | 1.22E+01 |
| 722 | 1.22E+01 | 0.59 | 1.84E+01 | 811 | 4.96E+00 | 0.54 | 8.44E+00 |
| 722 | 1.17E+01 | 0.58 | 1.84E+01 | 821 | 2.64E+00 | 0.59 | 3.98E+00 |
| 740 | 4.98E+00 | 0.65 | 6.71E+00 | 821 | 2.60E+00 | 0.58 | 3.99E+00 |
| 751 | 2.87E+00 | 0.64 | 3.91E+00 | 831 | 2.42E+00 | 0.58 | 3.73E+00 |
| 761 | 1.35E+00 | 0.65 | 1.83E+00 | 842 | 1.68E+00 | 0.57 | 2.69E+00 |
| 773 | 1.19E+00 | 0.63 | 1.69E+00 | 853 | 1.17E+00 | 0.58 | 1.80E+00 |
| 784 | 5.71E−01 | 0.61 | 8.36E−01 | 865 | 8.34E−01 | 0.63 | 1.16E+00 |
| 794 | 4.28E−01 | 0.63 | 5.99E−01 | 875 | 4.64E−01 | 0.63 | 6.50E−01 |
| 805 | 2.21E−01 | 0.64 | 3.05E−01 | 885 | 3.68E−01 | 0.62 | 5.18E−01 |
| 816 | 1.40E−01 | 0.63 | 1.97E−01 | 896 | 1.88E−01 | 0.62 | 2.67E−01 |
| 827 | 1.09E−01 | 0.62 | 1.56E−01 | 907 | 1.17E−01 | 0.63 | 1.63E−01 |
| 838 | 6.73E−02 | 0.64 | 9.17E−02 | 918 | 7.93E−02 | 0.61 | 1.15E−01 |
| 838 | 6.66E−02 | 0.66 | 8.76E−02 | 929 | 5.00E−02 | 0.62 | 7.13E−02 |
| 849 | 4.85E−02 | 0.63 | 6.73E−02 | 940 | 3.79E−02 | 0.63 | 5.31E−02 |
| 860 | 2.97E−02 | 0.65 | 4.00E−02 | 951 | 2.56E−02 | 0.63 | 3.59E−02 |
| 871 | 2.43E−02 | 0.63 | 3.42E−02 | 962 | 1.84E−02 | 0.65 | 2.45E−02 |
| 882 | 1.69E−02 | 0.63 | 2.38E−02 | 972 | 1.20E−02 | 0.64 | 1.65E−02 |
| 904 | 8.00E−03 | 0.63 | 1.12E−02 | 984 | 8.91E−03 | 0.66 | 1.18E−02 |
| 915 | 5.20E−03 | 0.65 | 6.98E−03 | 984 | 8.36E−03 | 0.62 | 1.18E−02 |
| 937 | 2.82E−03 | 0.64 | 3.84E−03 | 995 | 5.66E−03 | 0.64 | 7.78E−03 |
| 948 | 1.93E−03 | 0.63 | 2.63E−03 | 1006 | 4.80E−03 | 0.65 | 6.48E−03 |
| 969 | 1.16E−03 | 0.63 | 1.59E−03 | 1017 | 3.39E−03 | 0.64 | 4.64E−03 |
| 980 | 8.70E−04 | 0.64 | 1.17E−03 | 1028 | 2.84E−03 | 0.62 | 3.97E−03 |
| 1002 | 5.84E−04 | 0.63 | 7.86E−04 | 1038 | 1.54E−03 | 0.64 | 2.08E−03 |
| 1012 | 5.17E−04 | 0.65 | 6.76E−04 | 1049 | 1.08E−03 | 0.65 | 1.46E−03 |
| 1012 | 5.41E−04 | 0.65 | 7.13E−04 | 1060 | 7.96E−04 | 0.64 | 1.08E−03 |
| 1034 | 2.83E−04 | 0.64 | 3.73E−04 | 1071 | 5.57E−04 | 0.65 | 7.28E−04 |
| 1034 | 2.69E−04 | 0.60 | 3.86E−04 | 1071 | 6.09E−04 | 0.62 | 8.44E−04 |
| 1040 | 1.69E−04 | 0.62 | 2.29E−04 | 1082 | 7.01E−04 | 0.68 | 8.90E−04 |
| | | | | 1093 | 4.57E−04 | 0.64 | 6.20E−04 |
| | | | | 1104 | 3.79E−04 | 0.67 | 4.85E−04 |
| | | | | 1116 | 2.83E−04 | 0.64 | 3.77E−04 |
| | **Jadeite (jd)** | | | | **$jd_{66}ne_{33}$** | | |
| 816 | 6.44E+00 | 0.57 | 1.03E+01 | 770 | 1.37E+01 | 0.53 | 2.39E+01 |
| 827 | 3.64E+00 | 0.56 | 5.88E+00 | 781 | 1.15E+01 | 0.56 | 1.86E+01 |
| 838 | 2.29E+00 | 0.56 | 3.72E+00 | 781 | 9.60E+00 | 0.52 | 1.80E+01 |
| 838 | 2.30E+00 | 0.57 | 3.72E+00 | 792 | 4.64E+00 | 0.54 | 7.93E+00 |
| 849 | 1.31E+00 | 0.57 | 2.09E+00 | 802 | 2.17E+00 | 0.58 | 3.38E+00 |
| 859 | 7.63E−01 | 0.57 | 1.20E−00 | 803 | 2.26E+00 | 0.57 | 3.60E+00 |
| 860 | 7.66E−01 | 0.57 | 1.22E+00 | 814 | 1.73E+00 | 0.57 | 2.76E+00 |
| 870 | 6.64E−01 | 0.59 | 1.01E+00 | 824 | 1.23E+00 | 0.59 | 1.86E+00 |
| 871 | 4.64E−01 | 0.60 | 6.86E−01 | 836 | 7.20E−01 | 0.60 | 1.05E+00 |
| 881 | 3.73E−01 | 0.60 | 5.58E−01 | 847 | 4.24E−01 | 0.59 | 6.32E−01 |
| 881 | 3.09E−01 | 0.59 | 4.66E−01 | 858 | 2.65E−01 | 0.59 | 3.96E−01 |
| 892 | 2.27E−01 | 0.60 | 3.37E−01 | 864 | 1.54E−01 | 0.59 | 2.32E−01 |
| 903 | 1.75E−01 | 0.59 | 2.66E−01 | 880 | 9.93E−02 | 0.60 | 1.48E−01 |
| 903 | 1.33E−01 | 0.61 | 1.93E−01 | 891 | 6.36E−02 | 0.59 | 9.60E−02 |
| 903 | 1.41E−01 | 0.61 | 2.04E−01 | 897 | 3.70E−02 | 0.59 | 5.59E−02 |
| 903 | 1.59E−01 | 0.61 | 2.34E−01 | 912 | 2.15E−02 | 0.58 | 3.27E−02 |
| 914 | 1.24E−01 | 0.59 | 1.90E−01 | 923 | 1.66E−02 | 0.59 | 2.48E−02 |
| 915 | 8.31E−02 | 0.61 | 1.20E−01 | 930 | 9.13E−03 | 0.60 | 1.34E−02 |
| 924 | 7.24E−02 | 0.61 | 1.05E−01 | 945 | 8.40E−03 | 0.59 | 1.24E−02 |
| 925 | 5.48E−02 | 0.62 | 7.91E−02 | 954 | 3.44E−03 | 0.59 | 5.07E−03 |
| 936 | 4.03E−02 | 0.63 | 5.63E−02 | 956 | 3.44E−03 | 0.58 | 5.26E−03 |
| 936 | 3.82E−02 | 0.63 | 5.33E−02 | 956 | 3.47E−03 | 0.59 | 5.22E−03 |
| 946 | 2.49E−02 | 0.64 | 3.44E−02 | 963 | 2.89E−03 | 0.61 | 4.20E−03 |
| 947 | 3.28E−02 | 0.65 | 4.43E−02 | 976 | 1.74E−03 | 0.61 | 2.46E−03 |
| 958 | 1.51E−02 | 0.64 | 2.09E−02 | 978 | 2.08E−03 | 0.62 | 2.92E−03 |
| 968 | 1.13E−02 | 0.65 | 1.52E−02 | 987 | 1.52E−03 | 0.58 | 2.28E−03 |
| 979 | 1.30E−02 | 0.68 | 1.67E−02 | 998 | 8.29E−04 | 0.59 | 1.25E−03 |
| 990 | 6.34E−03 | 0.65 | 8.52E−03 | 1009 | 8.16E−04 | 0.60 | 1.14E−03 |
| 999 | 3.26E−03 | 0.61 | 4.72E−03 | 1020 | 4.63E−04 | 0.58 | 6.97E−04 |
| 1001 | 4.97E−03 | 0.65 | 6.65E−03 | 1022 | 4.72E−04 | 0.60 | 6.63E−04 |
| 1010 | 6.59E−03 | 0.66 | 8.70E−03 | 1031 | 5.31E−04 | 0.66 | 6.78E−04 |
| 1012 | 3.40E−03 | 0.67 | 4.38E−03 | 1033 | 4.76E−04 | 0.63 | 6.10E−04 |
| 1021 | 1.87E−03 | 0.61 | 2.67E−03 | 1043 | 4.84E−04 | 0.71 | 5.80E−04 |
| 1032 | 2.81E−03 | 0.64 | 3.85E−03 | 1044 | 4.23E−04 | 0.64 | 5.32E−04 |
| 1043 | 1.08E−03 | 0.60 | 1.55E−03 | 1053 | 1.90E−04 | 0.64 | 2.41E−04 |
| 1054 | 1.22E−03 | 0.61 | 1.74E−03 | 1054 | 3.87E−04 | 0.70 | 4.63E−04 |
| 1065 | 7.54E−04 | 0.62 | 1.01E−03 | 1055 | 3.71E−04 | 0.76 | 4.02E−04 |
| 1076 | 5.98E−04 | 0.61 | 8.57E−04 | 1064 | 1.67E−04 | 0.67 | 1.99E−04 |
| 1087 | 4.57E−04 | 0.62 | 6.28E−04 | 1075 | 1.50E−04 | 0.63 | 1.84E−04 |
| 1095 | 2.74E−04 | 0.65 | 3.38E−04 | | | | |

*Continued next page*

**TABLE 2**—*Continued*

| $T$, °C | $\tau^{l}_{P,T}$, s | β | $\langle\tau^{l}_{P,T}\rangle$, s |
|---|---|---|---|
| | $jd_{33}ne_{66}$ | | |
| 794 | 1.04E+01 | 0.51 | 1.97E+01 |
| 804 | 4.72E+00 | 0.53 | 8.43E+00 |
| 816 | 3.41E+00 | 0.54 | 5.89E+00 |
| 827 | 1.32E+00 | 0.58 | 2.04E+00 |
| 828 | 1.62E+00 | 0.56 | 2.68E+00 |
| 828 | 1.46E+00 | 0.56 | 2.36E+00 |
| 839 | 8.96E−01 | 0.58 | 1.40E+00 |
| 850 | 4.48E−01 | 0.58 | 6.91E−01 |
| 862 | 2.55E−01 | 0.60 | 3.82E−01 |
| 872 | 1.92E−01 | 0.59 | 2.87E−01 |
| 872 | 1.97E−01 | 0.60 | 2.87E−01 |
| 883 | 8.31E−02 | 0.58 | 1.29E−01 |
| 884 | 1.16E−01 | 0.60 | 1.70E−01 |
| 884 | 9.41E−02 | 0.60 | 1.37E−01 |
| 894 | 6.26E−01 | 0.59 | 9.31E−02 |
| 894 | 4.36E−02 | 0.58 | 6.78E−02 |
| 894 | 4.37E−02 | 0.58 | 6.70E−02 |
| 905 | 2.92E−02 | 0.59 | 4.39E−02 |
| 916 | 1.94E−02 | 0.57 | 3.05E−02 |
| 920 | 1.12E−02 | 0.58 | 1.72E−02 |
| 930 | 9.54E−03 | 0.61 | 1.33E−02 |
| 940 | 5.53E−03 | 0.58 | 8.41E−03 |
| 951 | 3.39E−03 | 0.59 | 5.06E−03 |
| 963 | 1.81E−03 | 0.57 | 2.77E−03 |
| 974 | 1.41E−03 | 0.56 | 2.21E−03 |
| 975 | 1.46E−03 | 0.57 | 2.27E−03 |
| 985 | 1.24E−03 | 0.61 | 1.73E−03 |
| 996 | 5.39E−04 | 0.58 | 7.89E−04 |

### Experimental procedure

In our PCS experiments the relaxation times for longitudinal strain were measured isothermally above the glass transition within the temperature ranges 711–1040 °C (ab), 799–1116 °C ($ab_{50}jd_{50}$), 816–1095 °C (jd), 770–1075 °C ($jd_{66}ne_{33}$), and 794–996 °C ($jd_{33}ne_{66}$). At higher temperatures, a deformation of the polished surfaces of the sample took place, and in case of $jd_{66}ne_{33}$ and $jd_{33}ne_{66}$ surface recrystallization occurred thus rendering further measurements impracticable. A vertically polarized $Ar^{+}$ laserbeam (wavelength = 488 nm, power = 500 mW) was focused into the prismatic glass samples, which were mounted in an electrically heated furnace. The vertically polarized component of the scattered light from the sample was collected at an angle of 90° to the incident beam by a photomultiplier whose output was fed to a digital autocorrelator (Brookhaven, BI-9000 AT). The measured time correlation curves cover a time range of four to eight orders of magnitude. The duration of the measurements varied from 10 min to 8 h depending on the relaxation time of the supercooled liquid. The temperature was measured by a Pt-$Pt_{90}Rh_{10}$ thermocouple in contact with the sample. The thermocouple was checked against the melting points of NaCl, Ag, and Au. The accuracy of the measured temperatures is believed to be ± 2 K. The samples are purged during the measurement by a dry $N_2$ flow to prevent a rapid surface crystallization at higher temperatures.

## RESULTS AND DISCUSSION

### Temperature dependence of longitudinal strain relaxation times

Figure 1 shows longitudinal strain relaxation functions at 12 different temperatures for supercooled albite liquid, which are representative for all investigated compositions. The longitudinal strain relaxation time is shifted approximately five orders of magnitude within the temperature range 740–1034 °C. The solid lines represents a

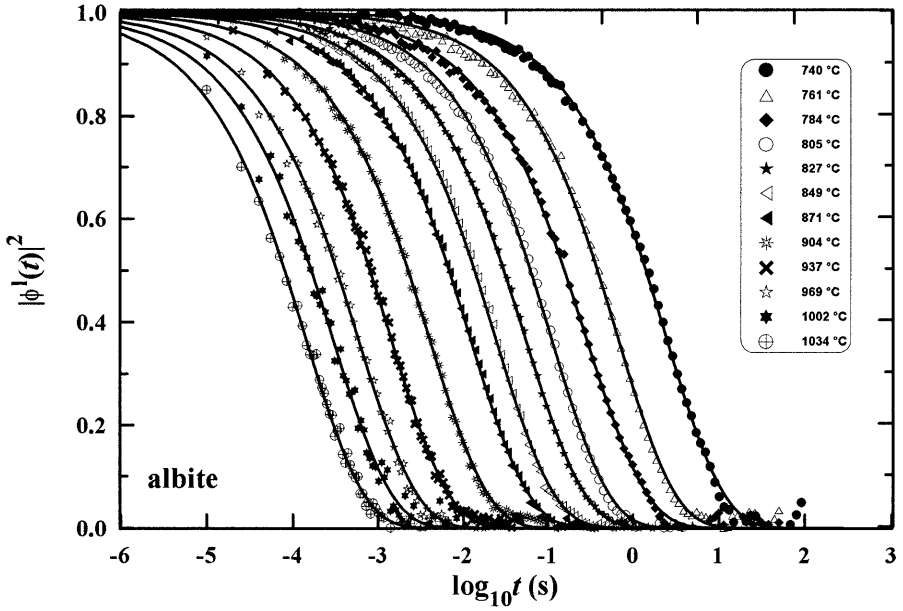


**FIGURE 1.** Longitudinal strain relaxation functions $|\Phi^{l}(t)|^2$ vs. $\log_{10}$ (time) for supercooled albite liquid at 12 temperatures. The solid lines are least squares fits using the Kohlrausch-Williams-Watts Equation 2.

**TABLE 3.** Activation energy $E_A$ and preexponent $\tau_0$ for longitudinal strain relaxation

| Composition | $T$ range (°C) | log $\tau_0$, s | $E_A$, kJ/mol |
|---|---|---|---|
| Albite (ab) | 711–1040 | −42.4 ± 0.5 | 372.3 ± 4.5 |
| $ab_{50}jd_{50}$ | 799–1116 | −44.7 ± 0.4 | 422.1 ± 3.9 |
| Jadeite (jd) | 816–1095 | −46.7 ± 0.6 | 441.7 ± 5.8 |
| $jd_{66}ne_{33}$ | 770–1075 | −49.7 ± 0.5 | 457.6 ± 5.2 |
| $jd_{33}ne_{66}$ | 794–996 | −59.7 ± 0.6 | 555.1 ± 5.9 |

least-squares fit to the Kohlrausch-Williams-Watts Equation 2.

The relaxation parameters $\langle\tau^l_{P,T}\rangle$, $\tau^l_{P,T}$, and β for all compositions at each temperature are summarized in Table 2. The standard deviation ($\pm 1\sigma$) of the least-squares fit is typically 0.5–2% for $\tau^l_{P,T}$ and β and 1–5% for $\langle\tau^l_{P,T}\rangle$, becoming larger for relaxation times slower than 5 s and faster than $10^{-3}$ s. The precision of the relaxation parameter ($\pm 1\sigma$), obtained from repeated measurements is ≤10% for $\tau^l_{P,T}$ and $\langle\tau^l_{P,T}\rangle$ and 3% for β.

The temperature dependence of the longitudinal strain relaxation times can be well described by an Arrhenian-type equation

$$\langle\tau^l_{P,T}\rangle = \tau_0 \exp\left(\frac{E_A}{RT}\right) \quad (4)$$

with $\tau_0$ = preexponent, $E_A$ = activation energy, $T$ = absolute temperature and R = universal gas constant. The values for $\tau_0$ and $E_A$ of each composition are listed in Table 3. Although a weak beginning of non-Arrhenian behavior for all compositions can be found, the relaxation time range of nearly 5 $\log_{10}$ units is too small to represent the temperature dependence of the data by the Vogel-Fulcher-Tamman (VFT) equation

$$\langle\tau^l_{P,T}\rangle = \tau_0 \exp\left(\frac{A}{T - T_0}\right) \quad (5)$$

with $\tau_0$ = preexponent and $A$, $T_0$ = constants. Relaxation times especially at higher temperatures are needed to extend the relaxation time range from 5 $\log_{10}$ units up to 8–12 $\log_{10}$ units. A determination of the non-Arrhenian behavior or ''fragility'' (Angell 1988) of the supercooled liquids by the equation of Sethna (1988)

$$\langle\tau^l_{P,T}\rangle = \exp\left(\frac{DT_0}{T - T_0}\right) \quad (6)$$

where D characterizes the fragility of the liquid and $T_0$ is from the VFT Equation 5, is also not possible. Despite this, the increasing fragility of the liquids with increasing $NaAlSiO_4$ content of composition can be shown in Figure 2. Here, the term ''strong'' denotes that a liquid tends to obey the Arrhenian equation whereas the term ''fragile'' denotes a liquid with non-Arrhenian behavior (Angell 1988). It is interesting that the supercooled liquid of albite composition falls away from this sequence, which is expected between the compositions of $SiO_2$ and $ab_{50}jd_{50}$. The chemical composition of this sample departs from the ideal stoichiometric composition and exhibits an excess of about 0.5 wt% $Na_2O$. Because an 50 °C lower glass transition temperature is observed by DTA measurements, in comparison with a nearly stoichiometric albite glass (Knoche 1993), we believe that the non-stoichiometry of the composition causes the departures in the relaxation times.

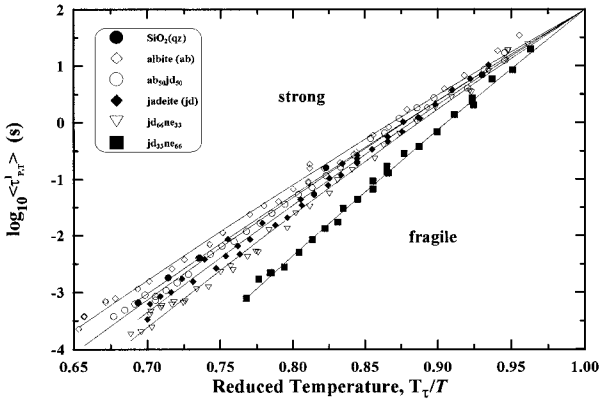


**FIGURE 2.** Temperature dependence of the longitudinal strain relaxation time $\langle\tau^l_{P,T}\rangle$ for the investigated supercooled liquids shown in the legend. The temperatures have been normalized to the temperature $T_\tau$, at which $\langle\tau^l_{P,T}\rangle$ = 100 s. These are 1214 °C ($SiO_2$), 679 °C (albite), 756 °C ($ab_{50}jd_{50}$), 763 °C (jadeite), 740 °C ($jd_{66}ne_{33}$), and 765 °C ($jd_{33}ne_{66}$).

## Thermorheological simplicity

A material is said to be thermorheological simple when the shape of its relaxation function is temperature independent (e.g., Scherer 1986), implying that the parameter β remains constant. Bucaro and Dardy (1977) pointed out that thermorheological simplicity (TRS) is an indicator for a temperature-independent structure within the valid temperature region. They argued that liquids that do not show TRS are those with a temperature-dependent structure. An example is supercooled $B_2O_3$ liquid, where a significant change in the shape of the longitudinal strain relaxation curves (Bucaro et al. 1975) correlates to a change in specific volume, expansivity (Macedo et al. 1966), and compressibility (Bucaro and Dardy 1974b). In contrast to $B_2O_3$, supercooled $SiO_2$ liquid shows TRS for longitudinal strain relaxation (Bucaro and Dardy 1977), has constant adiabatic moduli (Bucaro and Dardy 1974a), and has constant equilibrium compressibility (Bucaro and Dardy 1976), valid from the glass transition up to 1800 °C. However, in situ Raman spectroscopic studies of supercooled $SiO_2$ liquid up to 1950 K (McMillan et al. 1994) indicate a decrease in the average Si-O-Si angle with increasing temperature, which is interpretated as configurational changes of the structure.

Our data allow a further inspection regarding the statement of Bucaro and Dardy (1977) that TRS is an indicator for a temperature independent structure. It is evident from Figure 1 that the shape of the longitudinal strain relaxation curves of supercooled albite liquid are

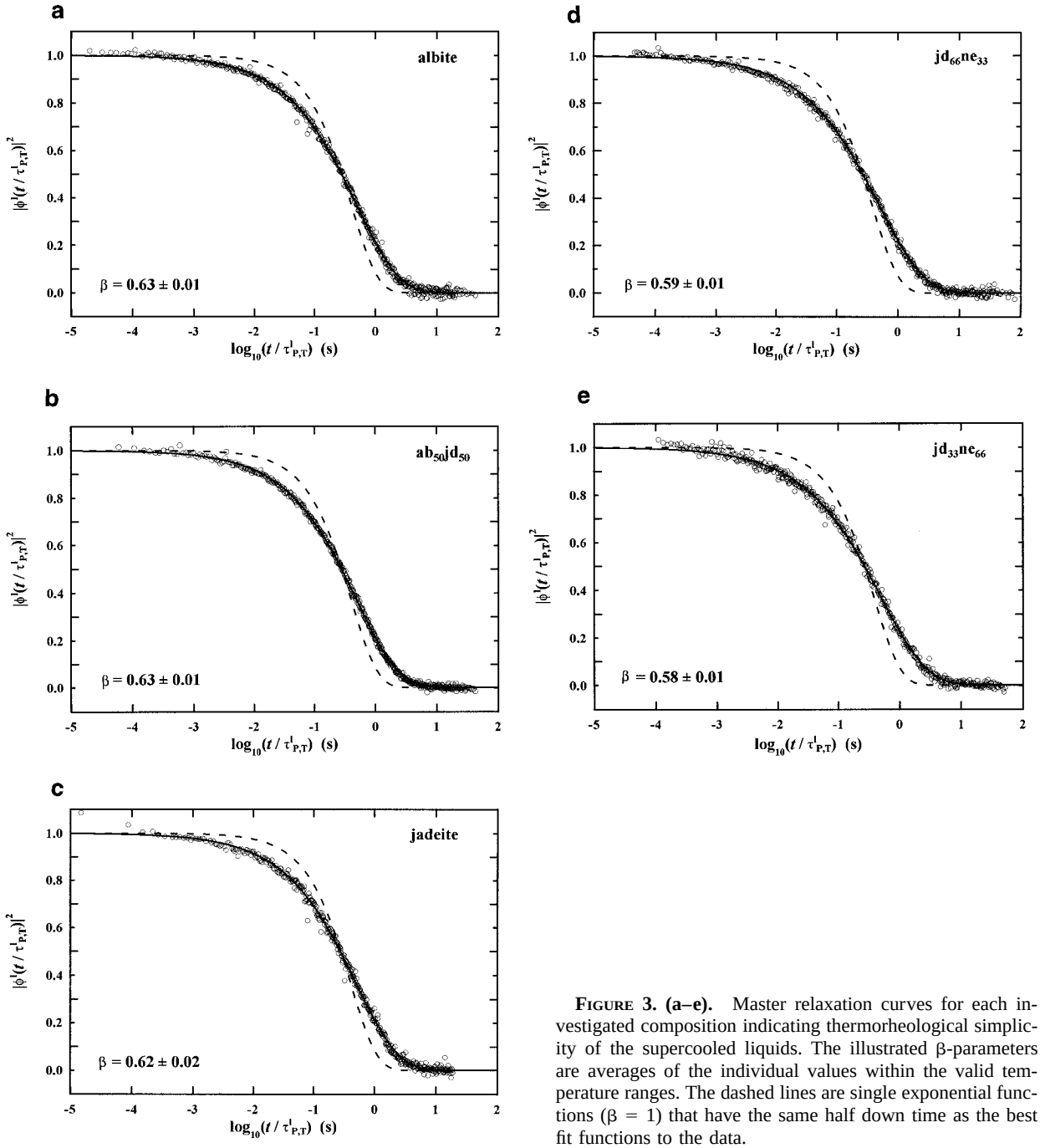


**FIGURE 3. (a–e).** Master relaxation curves for each investigated composition indicating thermorheological simplicity of the supercooled liquids. The illustrated β-parameters are averages of the individual values within the valid temperature ranges. The dashed lines are single exponential functions (β = 1) that have the same half down time as the best fit functions to the data.

similar and temperature independent. The curves are only shifted on the time scale, clearly indicating TRS behavior of the liquid corresponding to a constant β value within error. Normalization of the individual relaxation curves with respect to $\tau^{l}_{P,T}$ yields a master relaxation curve, which is shown for each composition in Figures 3a–e. TRS is not found within the whole investigated temperature range for all compositions but ranges from 740–1040 °C for ab, 865–1116 °C for $ab_{50}jd_{50}$, 870–1095 °C for jd, 802–1022 °C for $jd_{66}ne_{33}$, and 827–996 °C for $jd_{33}ne_{66}$. Especially at low temperatures the β values are lower (Table 2), which we attribute to a higher inaccuracy of the relaxation curves. An interpretation of these differences as a result of structural changes or a change of the relaxation mechanism seems to be too uncertain. Daniel et al. (1995) could not find any configurational changes up to 2000 K for albite melt and supercooled liquid using in situ Raman spectroscopy. So in this case the Raman spectroscopy study agrees with the result from relaxation

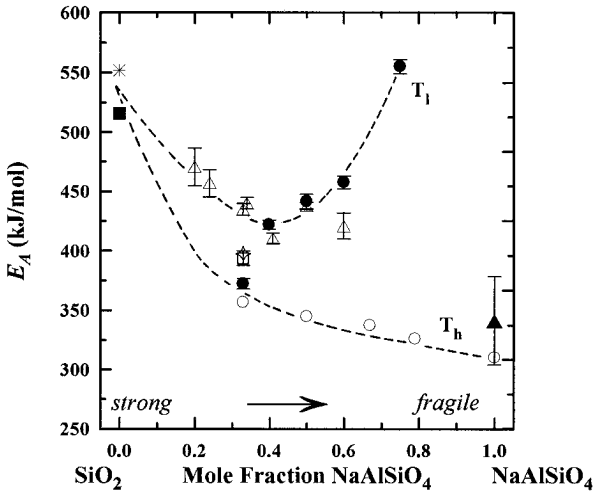


**FIGURE 4.** Composition dependence of the activation energies for strain relaxation and shear viscosity. Data sources: low temperature range = $T_l$; ● = this work, temperature range 711–1116 °C; □ = Knoche (1993), 717–806 °C; ◊ = Cranmer and Uhlmann (1981), 800–1000 °C. High temperature range = $T_h$: ○ = Riebling (1966) 1500–1680 °C; ▲ = N'Dala et al. (1984), 1594–1728 °C. Low and high-temperature range: Bucaro and Dardy (1977), 1305–1750 °C; ■ = Urbain et al. (1982), 1192–2482 °C. Intermediate temperature range: △ = Stein and Spera (1993) 1000–1300 °C. For better clarity the data of Taylor and Rindone (1970) and Hummel and Arndt (1985) are not presented, because they have a large deviation in comparison with the other values.

measurements, supporting the view that TRS is an indicator for a temperature-independent structure.

From Figures 3a–e it is also evident that the longitudinal strain relaxation processes of the investigated supercooled liquids cannot be described by a single relaxation time but by a distribution of relaxation times, indicated by $\beta < 1$. Several measurements on viscoelastic liquids show that volume, shear, and longitudinal relaxation processes are characterized by a distribution of relaxation times (Litovitz and Macedo 1965). It is assumed that the distribution of relaxation times derives from a cooperative inherently nonexponential rearrangement of the average configuration of the liquid (e.g., Moynihan et al. 1976).

### Dependence of activation energies on composition

According to the theory of viscoelasticity a comparison of the temperature dependence of strain relaxation times with that of shear viscosity is valid. Moreover, Lai et al. (1975) and Bucaro and Dardy (1977) showed that the activation energies resulting from strain relaxation times and shear viscosity data are of the same magnitude within error. Here, we compare activation energies obtained from strain relaxation times (Bucaro and Dardy 1977; this work) with activation energies from shear viscosity data (Riebling 1966; Taylor and Rindone 1970; Cranmer and Uhlmann 1981; Urbain et al. 1982; N'Dala et al. 1984; Hummel and Arndt 1985; Knoche 1993 and Stein and Spera 1993). Figure 4 shows the activation energy in the system $SiO_2$-$NaAlSiO_4$ as a function of composition. The derived activation energies correspond to two temperature ranges: a low-temperature range ($T_l$), with $T_g < T_l < T_g + 350$ °C ($T_g$ = glass transition temperature), and a high-temperature range ($T_h$), with $T_g + 750 < T_h < T_g + 1350$ °C. In the low-temperature region the activation energy passes through a minimum at ~40 mol% $NaAlSiO_4$, whereas in the high-temperature region the activation energy decreases with increasing $NaAlSiO_4$ content. We interpret this behavior to indicate increasing fragility toward $NaAlSiO_4$ composition, leading to a high activation energy at low temperatures and a low activation energy at high temperatures.

For supercooled albite liquid a significant scatter in the activation energies is found from literature, ranging from 557 kJ/mol (Taylor and Rindone 1970) through 500 kJ/mol (Hummel and Arndt 1985) down to 372 kJ/mol (this work). We assume that changes in the chemical composition could be responsible for this scatter, which is supported by an increase in the activation energy from 394 kJ/mol to 440 kJ/mol with decreasing Na/Al ratio from 1.07 to 0.95 from shear viscosity measurements for supercooled albite liquid (Knoche 1993). This could probably also explain the different activation energies found for supercooled jadeite liquid from Taylor and Rindone (1970) with 545 kJ/mol in comparison with this study (442 kJ/mol).

### Dependence of the parameter β and the excess (configurational) heat capacity $\Delta C_P$ on composition

Generally, fragile liquids are characterized by a large value of the excess (configurational) heat capacity, $\Delta C_P$, and tend to have relaxation processes with a broader distribution of relaxation times than strong liquids (Angell 1988). This means that β decreases with increasing $\Delta C_P$. Figure 5 represents the excess (configurational) heat capacity obtained from calorimeter measurements (Richet and Bottinga 1984; Martens et al. 1987), clearly indicating an increase of $\Delta C_P$ with increasing $NaAlSiO_4$ content and therefore increasing fragility. PCS measurements allow a very good determination of the parameter β, and the results are plotted along the join $SiO_2$-$NaAlSiO_4$ in Figure 6. The parameter β clearly decreases with increasing fragility. Moreover, from Figure 6 it seems that the relaxation time distribution derived from longitudinal strain relaxation measurements (Bucaro and Dardy 1977; this work) are broader than from enthalpy relaxation measurements (Richet and Bottinga 1984; Martens et al. 1987). A lower value for β obtained from viscoelastic relaxation in comparison with structural relaxation is also observed for $NaKSi_3O_7$, $B_2O_3$, and 5-phenyl 4-ether supercooled liquid (Moynihan et al. 1976). However, Angell (1988) found a lower value of β from enthalpy relaxation than from viscoelastic relaxation for a supercooled liquid with $3KNO_3 \cdot 2Ca(NO_3)_2$ composition.

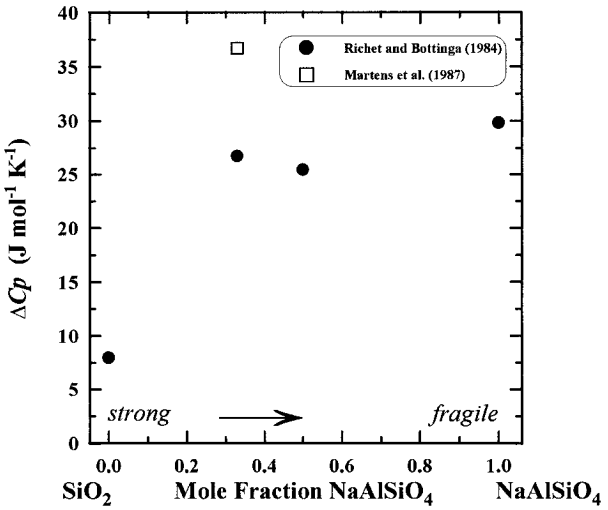


**FIGURE 5.** Composition dependence of the excess (configurational) heat capacity $\Delta C_P$, calculated from $\Delta C_P = C_{P,\text{melt}} - C_{P,\text{glass}}$ at the glass transition temperature.

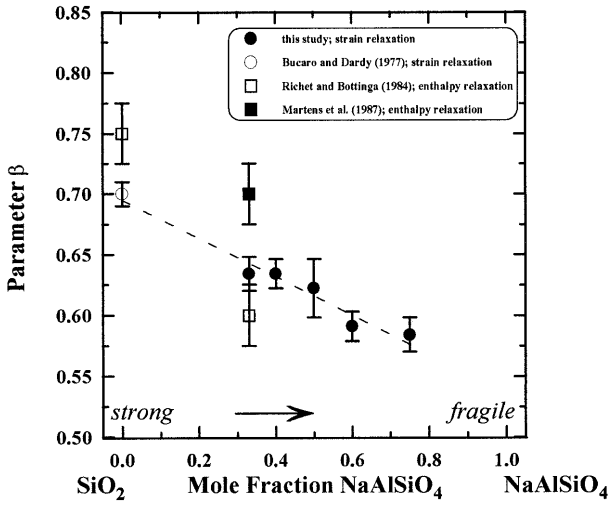


**FIGURE 6.** Composition dependence of the parameter β. The dashed line is a linear fit to PCS measurements including data for $SiO_2$ (Bucaro and Dardy 1977) and NaAl-silicates (this work) along the join $SiO_2$-$NaAlSiO_4$.

### Comparison of relaxation times for different properties

In this section we compare the time scales of relaxation processes for a given liquid recorded in terms of different properties. Generally, viscoelastic relaxation is the time-dependent response of a material to a mechanical load and can be subdivided into strain relaxation and stress relaxation. The average longitudinal strain relaxation time at constant stress and temperature, $\langle\tau^{l}_{P,T}\rangle$, is obtained from PCS measurements, whereas the average shear stress relaxation time at constant strain and entropy, $\langle\tau^{\text{sh}}_{\text{St},S}\rangle$, can be calculated from shear viscosity data by the Maxwell equation

$$\langle\tau^{\text{sh}}_{\text{St},S}\rangle = \frac{\eta_{\text{sh}}}{G_\infty} \tag{7}$$

with $\eta_{\text{sh}}$ = shear viscosity and $G_\infty$ = shear modulus (Herzfeld and Litovitz 1965; Bucaro and Dardy 1977). The relaxation time superscripts l and sh indicate longitudinal and shear, respectively, while the subscripts *P*, St, *T*, and *S* indicate constant stress, strain, temperature, and entropy, respectively. Strain relaxation times are, in general, different from stress relaxation times (e.g., Moynihan et al. 1976; Bucaro and Dardy 1977). Montrose et al. (1968) related these by

$$\langle\tau^{l}_{P,T}\rangle = \left(\frac{M_\infty}{M_0}\right)\langle\tau^{l}_{\text{St},T}\rangle, \tag{8}$$

with $M_0$ and $M_\infty$ = longitudinal modulus of the relaxed (0) and unrelaxed melt (∞), respectively. Until now the longitudinal moduli $M_0$ and $M_\infty$ in the system $SiO_2$-$NaAlSiO_4$ are only available for $SiO_2$.

In constrast to viscoelastic relaxation, structural relaxation is a time-dependent process according to a change in temperature. It is noteworthy that for a soda-lime-silicate liquid the hydrostatic stress required to produce a structural change equivalent to a temperature change of 1 °C is 12 MPa (Scherer 1986 p. 13). Therefore, for moderate stresses, the structural changes caused by a mechanical perturbation do not affect the viscosity, whereas a thermal perturbation may. Structural relaxation times can be obtained, for example, from dynamic heat capacity measurements, where the enthalpy relaxation is recorded. Here, the enthalpy relaxation time $\tau_{\text{H}}$ is given by the Tool-Narayanaswamy (TN) equation

$$\tau_H = A \exp\left[x\frac{\Delta h^*}{\text{R}T} + (1 - x)\frac{\Delta h^*}{\text{R}\cdot T_f}\right] \tag{9}$$

with $A$ = preexponent, $x$ ($0 \le x \le 1$) = nonlinearity parameter, $\Delta h^*$ = activation enthalpy, R = universal gas constant and $T_f$ = fictive temperature. Similar to longitudinal strain relaxation, enthalpy relaxation cannot be described by a single relaxation time, so that the average relaxation time of the relaxation time distribution has to be calculated by the gamma function with

$$\langle\tau_H\rangle = (\tau_H/\beta)\Gamma(1/\beta). \tag{10}$$

The equivalence between viscoelastic and structural relaxation times is discussed controversially in the literature. Rekhson (1975) showed for a variety of glasses, including $SiO_2$, $GeO_2$, and window glass, that the structural relaxation time at the glass transition temperature is larger than the stress relaxation time obtained by the Maxwell Equation 7 by a factor of 4–20. A difference in the relaxation kinetics of viscoelastic and structural relaxation has also been found for supercooled 5-phenyl 4-ether, $B_2O_3$, $NaKSi_3O_7$, and $As_2Se_3$ liquids (Moynihan et al. 1976), supercooled $3KNO_3{\cdot}2Ca(NO_3)_2$ liquid (Angell 1988), and supercooled jadeite liquid (Siewert and Rosenhauer 1994). However, Webb (1992), Stevenson et al. (1995), and Webb and Knoche (1996) found no dif-

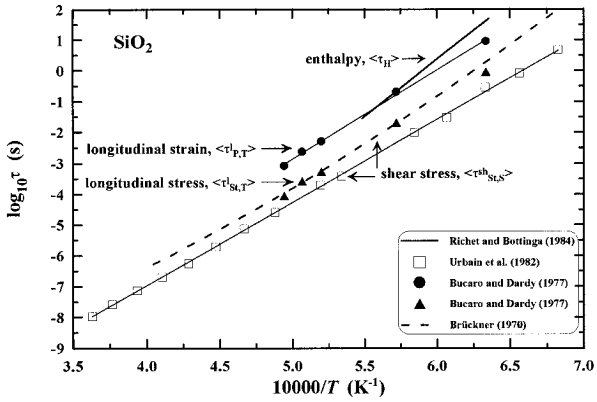


**FIGURE 7.** Comparison between enthalpy, shear, and longitudinal stress and longitudinal strain relaxation times for $SiO_2$ melt and supercooled liquid.

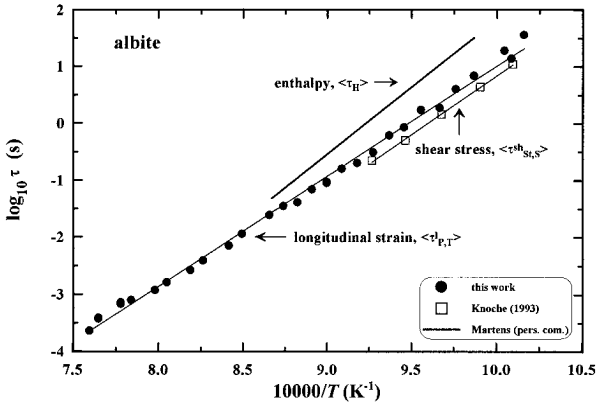


**FIGURE 8.** Comparison between enthalpy, shear stress, and longitudinal strain relaxation times for supercooled albite liquid.

ferences between enthalpy and shear stress relaxation times for several silicate melt compositions. These authors use a shear modulus value for $\log_{10} G_\infty$ of 10 ± 0.5 Pa for calculating the shear stress relaxation times by Equation 7, which is assumed to be an average value for silicate melts (Dingwell and Webb 1990). Consequently, any differences in the relaxation times are obscured by the large range of $G_\infty$ variation; in comparison, the observed differences between structural and viscoelastic relaxation time are within one or two $\log_{10}$ units.

Our data allow a further inspection with regard to a possible difference in the relaxation kinetics between structural and viscoelastic relaxation. Strain, stress, and enthalpy relaxation times for melt and supercooled liquid of $SiO_2$ and albite composition are represented in Figures 7 and 8, respectively. Here, shear stress relaxation times $\langle \tau^{sh}_{St,S} \rangle$ are calculated from shear viscosity data (Brückner 1970; Urbain et al. 1982; Knoche 1993) by means of Equation 7 using a measured value for $\log_{10} G_\infty$ of 10.5 Pa for $SiO_2$ (Bucaro and Dardy 1974a) and the average value of silicate melts for $\log_{10} G_\infty$ of 10 ± 0.5 Pa for albite composition. The enthalpy relaxation times for supercooled albite (Martens, personal communication) and $SiO_2$ liquid (Richet and Bottinga 1984) are calculated by Equations 9 and 10. It is evident that for supercooled $SiO_2$ and albite liquid the enthalpy relaxation time is slower than any of the viscoelastic relaxation times. It is important to mention that the samples of albite composition used for dynamic heat capacity, shear viscosity, and longitudinal strain relaxation measurements are from the same batch, so that an influence on the relaxation time because of slight differences in composition can be excluded. In contrast to albite, the measurements on vitreous $SiO_2$ were made with different samples. Different OH contents of the samples of vitreous $SiO_2$ may be the reason for the differences between the shear viscosity data from Brückner (1970) and Urbain et al. (1982), because the OH content has a strong influence on the viscosity of vitreous $SiO_2$ (Brückner 1970). We believe that the difference in the relaxation times may be interpreted as meaning that structural relaxation is associated with major configurational changes such as bond breaking, whereas viscoelastic relaxation involves stretching and aligning of bonds or structural units. This could also explain the different values for the parameter β of structural and viscoelastic relaxation.

## ACKNOWLEDGMENTS

This paper is dedicated to the memory of Matthias Rosenhauer, who died February 10, 1996. He initiated the research on relaxation measurements of silicate melts at the University of Göttingen. His friendly leadership, his contagious enthusiasm, and his readiness to discuss at any time are greatly missed. Many thanks to K. Roselieb and S. Foley for helpful suggestions and to C.T. Moynihan and an anonymous reviewer for constructive comments. This research was supported by a grant of the Deutsche Forschungsgemeinschaft (Ro 414/15-1).

## REFERENCES CITED

Angell, C.A. (1988) Structural instability and relaxation in liquid and glassy phases near the fragile liquid limit. Journal of Non-Crystalline Solids, 102, 205–221.

Berne, B.J. and Pecora, R. (1976) Dynamic light scattering, 400 p. Wiley, New York.

Brückner, R. (1970) Properties and structure of vitreous silica. Journal of Non-Crystalline Solids, 5, 123–175.

Bucaro, J.A. and Dardy, H.D. (1974a) High-temperature brillouin scattering in fused quartz. Journal of Applied Physics, 45, 5324–5329.

——— (1974b) Light scattering from boron trioxide through the glass transition. Journal of Applied Physics, 45, 2121–2124.

——— (1976) Equilibrium compressibility of glassy $SiO_2$ between the transformation and melting temperature. Journal of Non-Crystalline Solids, 20, 149–191.

——— (1977) High-temperature strain relaxation in silica by optical correlation spectroscopy. Journal of Non-Crystalline Solids, 24, 121–129.

Bucaro, J.A., Dardy, H.D., and Corsaro, R.D. (1975) Strain relaxation in glass by optical correlation and pressure jump relaxation. Journal of Applied Physics, 46, 741–746.

Cranmer, D. and Uhlmann, D.R. (1981) Viscosity of liquid albite, a network material. Journal of Non-Crystalline Solids, 45, 283–288.

Daniel, I., Gillet, P., Poe, B.T., and McMillan, P.F. (1995) In-situ high-temperature Raman spectroscopic studies of aluminosilicate liquids. Physics and Chemistry of Minerals, 22, 74–86.

Dingwell, D.B. and Webb, S.L. (1990) Structural relaxation in silicate melts. European Journal of Mineralogy, 2, 427–449.

Herzfeld, K.F. and Litovitz, T.A. (1965) Absorption and dispersion of ultrasonic waves, p. 473. Academic Press, New York.

Höfler, S. and Seifert, F.A. (1984) Volume relaxation of compacted $SiO_2$-glass: a model for the conversation of natural diaplectic glasses. Earth and Planetary Science Letters, 67, 433–438.

Hummel, W. and Arndt, J. (1985) Variation of viscosity with temperature and composition in the plagioclase system. Contributions to Mineralogy and Petrology, 90, 83–92.

Knoche, R. (1993) Temperaturabhängige Eigenschaften silikatischer Schmelzen. Untersuchungen in den Systemen $Na_2O$-$SiO_2$ und $NaAlSi_3O_8$-$CaAl_2Si_2O_8$-$CaMgSi_2O_6$, 186 p. Ph.D. thesis, Universität Bayreuth, Germany.

Lai, C.C., Macedo, P.B., and Montrose, C.J. (1975) Light-scattering measurements of structural relaxation in glass by digital correlation spectroscopy. Journal of the American Ceramic Society, 58, 120–123.

Litovitz, T.A. and Macedo, P. (1965) Ultrasonic relaxation, viscosity and free volume in molten glasses. In J.A. Prins, Ed., Physics of non-crystalline solids, Proceedings of the International Conference, p. 220–230. North-Holland Publishing Co., Amsterdam.

Macedo, P.B., Capps, W., and Litowitz, T.A. (1966) Two-state model for the free volume of vitreous $B_2O_3$. Journal of Chemical Physics, 44, 3357–3364.

Martens, R.M., Rosenhauer, M., Büttner, H., and Von Gehlen, K. (1987) Heat capacity and kinetic parameters in the glass transformation interval of diopside, anorthite and albite glass. Chemical Geology, 62, 49–70.

Mazurin, O.V. (1986) Glass relaxation. Journal of Non-Crystalline Solids, 87, 392–407.

McMillan, P.F., Poe, B.T., Gillet, P., and Reynard, B. (1994) A study of $SiO_2$ glass and supercooled liquid to 1950 K via high-temperature raman spectroscopy. Geochimica et Cosmochimica Acta, 58, 3653–3664.

Mills, J.J. (1974) Low frequency storage and loss moduli of soda-silica glasses in the transformation range. Journal of Non-Crystalline Solids, 14, 255–268.

Montrose, C.J., Solovyev, V.A., and Litovitz, T.A. (1968) Brillouin scattering and relaxation in liquids. Journal of the Acoustical Society of America, 43, 117–130.

Moynihan, C.T., Macedo, P.B., Montrose, C.J., Gupta, P.K., DeBolt, M.A., Dill, J.F., Dom, B.E., Drake, P.W., Easteal, A.J., Elterman, P.B., Moeller, R.P., Sasabe, H., and Wilder, J.A. (1976) Structural relaxation in vitreous materials. Annals New York Academy of Sciences, 279, 15–35.

Mysen, B.O. (1988) Structure and properties of silicate melts, 354 p. Elsevier, Amsterdam.

N'Dala, I., Cambier, F., Anseau, M.R., and Urbain, G. (1984) Viscosity of liquid feldspars: I. Viscosity measurements. British Ceramic Transactions and Journal, 83, 105–107.

Rekhson, S.M. (1975) Structural relaxation and shear stresses in the glass-transition region. Soviet Journal of Glass Physics and Chemistry, 1, 417–421.

Richet, P. and Bottinga, Y. (1984) Glass transitions and thermodynamic properties of amorphous $SiO_2$, $NaAlSi_nO_{2n+2}$ and $KAlSi_3O_8$. Geochimica et Cosmochimica Acta, 48, 453–470.

Riebling, E.F. (1966) Structure of sodium aluminosilicate melts containing at least 50 mole % $SiO_2$ at 1500 °C. Journal of Chemical Physics, 44, 2857–2865.

Scherer, G.W. (1986) Relaxation in glass and composites, 331 p. Wiley, New York.

Sethna, J.P. (1988) Speculations on the glass transition. Europhysics letters, 6, 529–534.

Siewert, R. and Rosenhauer, M. (1994) Light scattering in jadeite melt: strain relaxation measurements by photon correlation spectroscopy. Physics and Chemistry of Minerals, 21, 18–23.

Stein, D.J. and Spera, F.J. (1993) Experimental rheometry of melts and supercooled liquids in the system $NaAlSiO_4$-$SiO_2$: Implications for structure and dynamics. American Mineralogist, 78, 710–723.

Stevenson, R.J., Dingwell, D.B., Webb, S.L., and Bagdassarov, N.S. (1995) The equivalence of enthalpy and shear stress relaxation in rhyolitic obsidians and quantification of the liquid-glass transition in volcanic processes. Journal of Volcanology and Geothermal Research, 68, 297–306.

Taylor, M. and Brown, G.E. (1979) Structure of mineral glasses: II. The $SiO_2$-$NaAlSiO_4$ join. Geochimica et Cosmochimica Acta, 43, 61–75.

Taylor, T.D. and Rindone, G.E. (1970) Properties of soda aluminosilicate glasses: V, low temperature viscosities. Journal of the American Ceramic Society, 53, 692–695.

Urbain, G., Bottinga, Y., and Richet, P. (1982) Viscosity of liquid silica, silicates and aluminosilicates. Geochimica et Cosmochimica Acta, 46, 1061–1072.

Webb, S.L. (1992) Shear, volume, enthalpy and structural relaxation in silicate melts. Chemical Geology, 96, 449–457.

Webb, S. and Knoche, K. (1996) The glass-transition, structural relaxation and shear viscosity of silicate melts. Chemical Geology, 128, 165–183.

Williams, G. and Watts, D.C. (1970) Non-symmetrical dielectric relaxation behaviour arising from a simple empirical decay function. Transactions of the Faraday Society, 66, 80–85.

Manuscript received November 14, 1996
Manuscript accepted July 23, 1997